International Journal of Innovation and Applied Studies
ISSN 2028-9324 Vol. 34 No. 3 Nov. 2021, pp. 521-531

http://www.ijias.issr-journals.org/

Modeling of Humidity Evolution During Solar Drying of Cassava in a Ventilated Attic

Aristide Tieu[1], Simon Abe Yapi[1], and Prosper Gbaha[2]

[1]Laboratoire de Technologie, Université Félix Houphouet-Boigny, 22 BP 582 Cocody Abidjan 22, Côte d'Ivoire

[2]Laboratoire d'Energie Nouvelle et Renouvelable, Institut National Polytechnique Félix Houphouet-Boigny, BP 581, Yamoussoukro, Côte d'Ivoire

ABSTRACT: In Africa, it is possible to take advantage of the heat provided by metal roofs (constantly exposed to the sun) for the drying of agricultural products to reduce post-harvest losses. For this purpose, a prototype ventilated attic equipped with shelves is built and tested on the drying of cassava. For 6 kg of manioc, it takes three days to dry in the prototype. The modeling of moisture growth in the drying air is carried out by the fourth-order Runge-Kutta method. The theoretical results allow predicting the variation of moisture in the air of the attic with accuracy. Modeling of the manioc drying curve is made using five semi-empirical models. The Midili-Kucuk model is the one that best predicts moisture content evolution in cassava, as it gives the highest value of the determination coefficient. As drying is a simultaneous heat and mass transfer phenomenon, the coefficients of heat and mass transfer evolutions were observed too. We noticed their increase with drying time. The presence of fresh products in the attic keeps its internal temperature lower than outside. When the products are no longer fresh, the temperature of the attic (on the products) increases. Polystyrene insulation on the ceiling, product bed and air circulation generated by chimneys help prevent heat from migrating through the ceiling. So, this attic has two advantages: the drying of products to extend its shelf life and reduction of heat in houses.

KEYWORDS: Runge-Kutta, modeling, solar drying, ventilated attic, drying air, drying curve.

1 INTRODUCTION

The issue of food drying, either to increase its market value or for its long-term preservation, is still current. It is the subject of several rather recent works. Indeed, for several developing countries and particularly for farmers in Africa, the appropriate methods of treatment for agricultural productions are unknown [1] and they face heavy post-harvest losses [2], [3], [4]. Drying is a critical step in preventing farm production losses [5]. Reference [6] studied the coefficient of shrinkage, the coefficient of moisture diffusion, and drying kinetic of cocoa in an indirect solar dryer. In another article [7], he establishes relationships to calculate the density, porosity, mass transfer coefficient, and heat transfer coefficient for the drying of the same product. Reference [8] introduced an indirect solar dryer for farm products and meat. He presented its economic benefits for users. Reference [9] exhibits in recent works, different types of solar dryers widely used in Africa and Asia. Their effects on product quality and the economic, environmental, and social impact are also exposed. Reference [10] presented different drying systems and the conditions of their use. He suggested that for efficient and economically viable drying, the design of the dryer should take into account the characteristics of the product to be dried as well as the climatic conditions in which the drying is carried out. Experimentation, in its implementation, is often costly. Several researchers are increasingly turning to the modeling of transfers that take place during the drying process [11], [12], [13], [14]. Reference [15] proposed a heat and mass transfers models for the drying of red chili in a natural-convection mixed-mode solar dryer. The differential equations of the model were solved numerically by the fourth-order Runge-Kutta method. The validation of the models was done by comparison of calculated data with experimental results. Several other models of agricultural drying have been carried out by researchers to facilitate understanding of the method [16], [17], [18], [19]. Drying in the attic is a very old technique always in use by the peasants of West Africa in remote places. The products to be dried are exposed in the attics of the huts whose roofs are made of straws, to keep them away from pets, thieves and dirt. Drying occurs under the effect of wood smoke or after a long period under the effect of the low airflow in the attic. The result is poor quality products infested with the taste, smell, and color of smoke or attacked by mold. The metal roofs, constantly exposed to the sun in Africa, are real sources of heat and they offer the possibility to improve this old technique of drying in the attic. For this purpose, a prototype attic ventilated with natural convection, which can be used to dry the agricultural products is built and tested. In this work, we undertake modeling of the variation in the water content of the drying air and the water content of the manioc used for drying. Changes in heat and mass transfer coefficients are observed. The advantages of the method for the thermal comfort of the houses are also presented.

2 Materials And Methods

2.1 Mass Balance Equations

The mass transfer on the air takes into account the humidity absorbed from the product surface by the air and the variation of humidity due to the variation of air absolute humidity values inside and outside the dryer [20], [21]. The mass balance is therefore applied to the manioc slices used as products to dry and to the drying air. Based on these assumptions, the mass transfer equation is given like this:

$$\mathrm{m_a Y_s}' = \dot{\mathrm{m}}(\mathrm{Y_e} - \mathrm{Y_s}) - \mathrm{m_0}\dot{\mathrm{X}} \tag{1}$$

The drying of manioc is usually done in two phases [22], [23]:

- The constant rate drying phase is generally considered as an adiabatic drying phase.
- The decreasing-rate period.

During the first drying phase (constant rate), the mass variation in the product can be expressed like this:

$$\dot{m_p} = \mathrm{m_0}\dot{\mathrm{X}} = \frac{\mathrm{h_c}}{\mathrm{L_v}}\mathrm{S_p}\left(\mathrm{T_a} - \mathrm{T_p}\right) \tag{2}$$

$\boldsymbol{h_c}$, $\boldsymbol{L_v}$, $\boldsymbol{T_a}$, $\boldsymbol{T_p}$ are heat transfer coefficient, latent heat of water vaporization, drying air temperature, and product temperature respectively. During the drying speed drop phase, the following equation was established for the moisture content $\mathrm{X_t}$ of the product:

$$\log\left(\frac{\mathrm{X_t} - \mathrm{X_f}}{\mathrm{C}}\right) = -\mathrm{at} \tag{3}$$

This allows us to write the following expressions:

$$\mathrm{X(t)} = \mathrm{C.e^{-at}} + \mathrm{X_f} \tag{4}$$

Then:

$$\mathrm{m_0}\dot{\mathrm{X}} = -\mathrm{a.m_0.Ce^{-at}} \tag{5}$$

The constant drying rate phase is brief and is not always seen. In this study, we only take into account the falling rate phase. For this phase, during the drying of cassava conducted by [23], the value of the constant "a" is 4.10^{-5}. We assume this value for our modeling. Constant "C" is the difference between the initial water content and the final water content of the product (experimentally determined). The inlet external air absolute water content is given by the following expression:

$$\mathrm{Y_e} = \frac{0.622}{\frac{\mathrm{P}}{\mathrm{Hr.Ps(T)}} - 1} \tag{6}$$

Where P is atmospheric pressure, it is given according to the altitude Z by the following expression [24] :

$$\mathrm{P} = 101325 - 12\mathrm{Z} + 5{,}2.10^{-4}\mathrm{Z}^2 \tag{7}$$

Hr is the measured air relative humidity and $Ps(T)$, the pressure of air in the saturated state, it is given by the Formula of Dupré :

$$\mathrm{Ps(T)} = e^{\left[46{,}784 - \frac{6435}{T+273{,}15} - -3{,}868.\ln(T+273{,}15)\right]} \quad (8)$$

T is the temperature (°C). Based on the attic air relative humidity values measured, the values of its experimental absolute humidity are determined. For the resolution of eq. (1) by the fourth-order Runge-Kutta method, it is written in the following form:

$$Y_s'(t) = \frac{\rho_a S v_a}{m_a}(Y_e(t) - Y_s) + \frac{m_0}{m_a} a.Ce^{-at} \quad (9)$$

Where ρ_a, S et v_a are respectively air density, attic air inlet surface, and the average airspeed.

Then we can write:

$$f(Y_{s,n}, t_n) = \frac{\rho_a S v_a}{m_a}\left(Y_e(t_n) - Y_{s,n}\right) + \frac{m_0}{m_a} a.Ce^{-at_n} \quad (10)$$

$Y_s(0) = 18.63\ g/kga.s$ (initial absolute humidity of drying air in the morning), t_0= 0, the step time is h = 15 minutes, the anhydrous mass of the cassava is $m_0 = 2.22\ kg$, air mass flow rate

$\dot{m} = \rho_a.S.v_a \approx 0.013\ kg/s.$

$$K_1 = h * f(Y_{s,n}, t_n) \quad (11)$$

$$K_2 = h * f\left(Y_{s,n} + \frac{K_1}{2}, t_n + \frac{h}{2}\right) \quad (12)$$

$$K_3 = h * f\left(Y_{s,n} + \frac{K_2}{2}, t_n + \frac{h}{2}\right) \quad (13)$$

$$K_4 = h * f(Y_{s,n} + K_3, t_n + h) \quad (14)$$

$$Y_{s,n+1} = Y_{s,n} + \frac{1}{6}(K_1 + 2K_2 + 2K_3 + K_4) \quad (15)$$

$$t_{n+1} = t_n + h \quad (16)$$

From a Matlab language R2014a, we get the theoretical values of the drying air absolute humidity. These values allow us to calculate its theoretical relative humidity values at any time.

2.2 Modeling Of Cassava Drying Curve

For the choice of the model that better describes the cassava drying curve, five semi-empirical models were used (Tab. 1). To evaluate the fitting performance, the following statistical parameters were used, namely: the coefficient of determination (R^2), the chi-square (χ^2), and the root mean square error (RMSE) [25], [26]. Their expressions are given below.

Table 1. Semi-empirical models used for cassava drying curve modeling

Names of the models	Expression of the moisture content
Newton	X(t)=exp(-kt)
Page	X(t) = exp (-kt^n)
Henderson and Pabis	X(t) = a.exp (-kt)
Logarithmic	X(t) = a.exp (-kt) + c
Midilli-Kucuk	X(t) = a.exp (-kt^n) + bt

Where a, k, n, b, and c are constants. The water content of the manioc is calculated from the values of the weight of the manioc obtained experimentally.

$$X(t) = \frac{m_t - m_0}{m_0} \quad (17)$$

m_t is the weight of the product at any time t.

$$R^2 = 1 - \left[\frac{\sum_{i=1}^{N}(X_{pre} - X_{exp})^2}{\sum_{i=1}^{N}(\bar{X}_{pre} - X_{exp})^2}\right] \quad (18)$$

$$\chi^2 = \frac{\sum_{i=1}^{N}(X_{pre} - X_{exp})^2}{N - Z} \quad (19)$$

$$RMSE = \left[\frac{1}{N}\sum_{i=1}^{N}\left(X_{pre} - X_{exp}\right)^2\right]^{1/2} \quad (20)$$

N: number of experimental points, Z is the number of constants.
X_{pre} : the predicted value of moisture content by the model and
X_{exp} : moisture content from experimental data.

2.3 HEAT TRANSFER AND MASS TRANSFER

Drying occurs in a process of simultaneous transfer of heat and mass between the product and the drying air. As established by [7], the heat transfer coefficient (h) and mass transfer coefficient (h_m) are expressed as follows:

$$h_m = \frac{V}{S_p t}\ln\left(\frac{X_0 - X_f}{X_t - X_f}\right) \quad (21)$$

$$h = \frac{\rho_a C_{pa} d_p}{6t} Le^{2/3} \ln\left(\frac{X_0 - X_f}{X_t - X_f}\right) \quad (21)$$

In these equations, X_0, X_f, and X_t are cassava initial, equilibrium and, instantaneous moisture content respectively. Le (≈ 0.85) is the Lewis number, V, S_p, d_p, are cassava slice volume, exchange surface, and diameter respectively. ρ_a is air density and C_{pa} is air's specific heat. t is the time elapsed. Cassava slices are parallelepipedic with approximately 40 mm length, 25 mm wide and 7 mm thick. So average volume is $\overline{V} = 7cm^3$. The average geometric diameter is deducted by the following method:

$$\bar{V} = \frac{4}{3} * \pi * \left(\frac{\overline{d_p}}{2}\right)^3 = \frac{\pi}{6} * \overline{d_p}^3 \quad (22)$$

So we can write

$$\overline{d_p} = \left(\frac{6\overline{V}}{\pi}\right)^{1/3} \quad (23)$$

2.4 DESCRIPTION OF THE PROTOTYPE VENTILATED ATTIC

The prototype ventilated attic used for the solar food drying (Fig. 1) is equipped with three PVC pipe chimneys, each 1,5 m high and 50 mm in diameter. The roof is made of an aluminum-zinc wavy sheet and it is blackened (as drying is energy demanding) to increase the heating of the products during the day thanks to the sun. The ceiling is 10 mm thick plywood and it is covered with a 8 cm thick polystyrene layer to prevent the heat from crossing it [27]. The drying shelves are arranged in staircase along the roof and separated by vertical boards to ensure uniform heating of the products; the boards prevent wet air from a shelf to go through the next. The prototype is 860 mm wide and 1.8 m long. The air inlet has a width of 840 mm and a height of 40 mm. Each drying shelf was charged with 1,5 kg of cassava. The prototype is tilted at a 10° angle compared to the horizontal plane. And the whole thing is mounted on a support of 2,5 m high to have a height of house roofs.

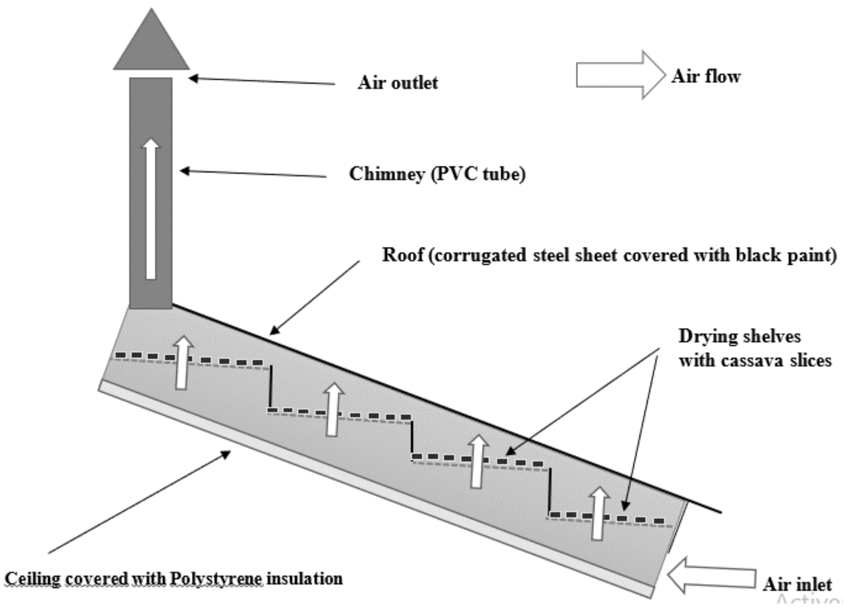

Fig. 1. Profile view of the ventilated attic prototype

3 Results And Discussion

3.1 Experimental Results

Fig. 2 shows evolution of both ambient air and attic's air relative humidity. The humidity of the ambient air varies from 32% and 76% for these three days of drying. For the air of the attic, its moisture ranges between 31,26% and 80,45%. On the first and second drying days, we can see that drying air relative humidity is higher than that of ambient air. Indeed, at the beginning of drying, manioc contains a lot of free water. This water is easily released into the attic's air with the diurnal increase of solar radiation. In the evening, with reduction of sunshine, moisture grows in attic's air as well as in the ambient air. Similar results were observed by Tagne [15] during drying of red chili in a mix-mode solar dryer. He noticed that air in the drying chamber was slightly wetter than air at the solar collector outlet. In our case, there is no air preheating system, therefore air in the prototype containing the fresh cassava is wetter.

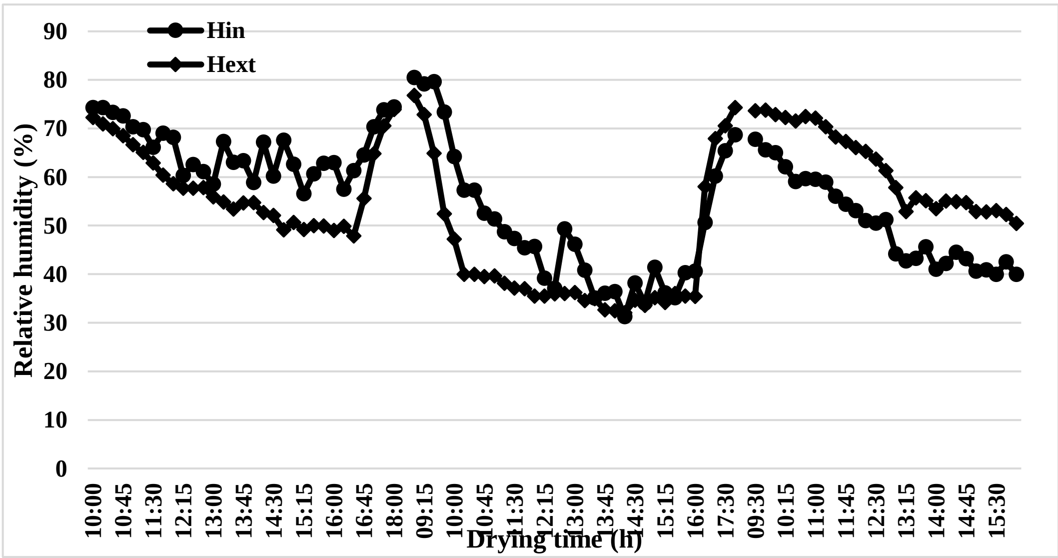

Fig. 2. Ambient air relative humidity (Hext) and attic's air relative humidity (Hin)

On the last drying day, humidity released by the product is very low because it is almost dried and the remaining moisture is increasingly bound in it. Then we can observe that drying air relative humidity is lower than that of ambient air whatever the sun intensity. These observations are consistent with the drying curve (Fig. 3). We can observe a rapid decrease in the moisture content during the first two drying days. On the last day, the drying is very slow and moisture doesn't decrease any more when it reaches the threshold value of 0.126kg/kg in dry basis.

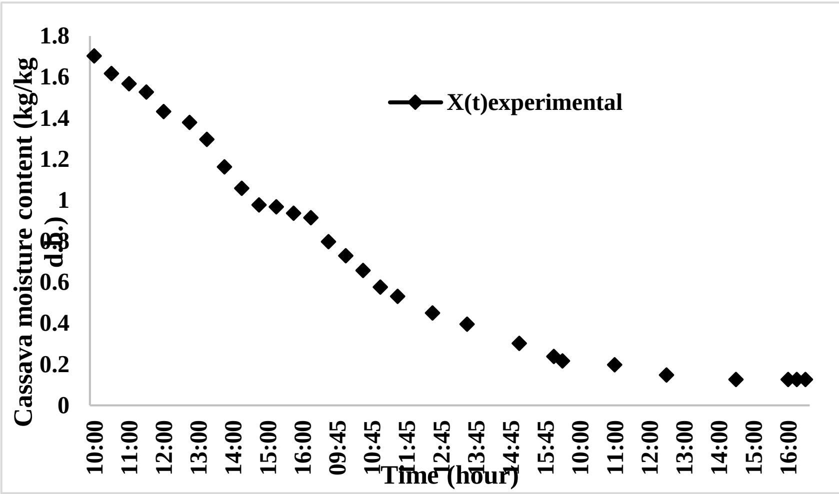

Fig. 3. Variation in moisture content of cassava during indirect solar drying in the attic

3.2 MODELING OF HUMIDITY EVOLUTION IN DRYING AIR

Fig. 4a presents the evolutions of experimental and numerical evolution of moisture in the drying air. The mean relative percentage deviation modulus [28], E%, was calculated to evaluate fit quality. It allows correlating the theoretical and experimental data. Low values (E%< 10%) are signs of good fit. It's expressed in the following way:

$$E\% = \frac{1}{N}\sum_{i=1}^{N}\frac{|Hr_{in\ exp}-Hr_{in\ theo}|}{Hr_{in\ exp}} \quad (25)$$

$Hr_{in\ exp}$: the experimental value of drying air relative humidity.
$Hr_{in\ theo}$: Theoretical value of drying air relative humidity.
N: number of observations

The value obtained for this modeling, E%= 6,9% is satisfactory, [4] obtained similar results for the modeling of temperature in the chimney of his dryer. It shows that this model can predict the evolution of moisture in the attic's air with accuracy. This statement is confirmed by the good distribution of the points around the X=Y line observed in Fig. 4b below.

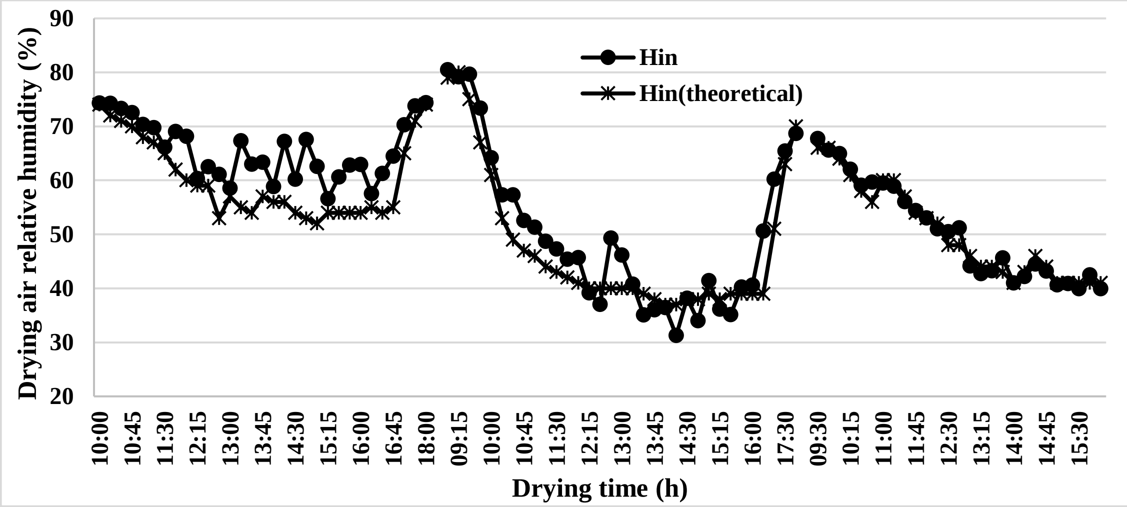

Fig. 4. a. Experimental and numerical drying air relative humidity versus drying time

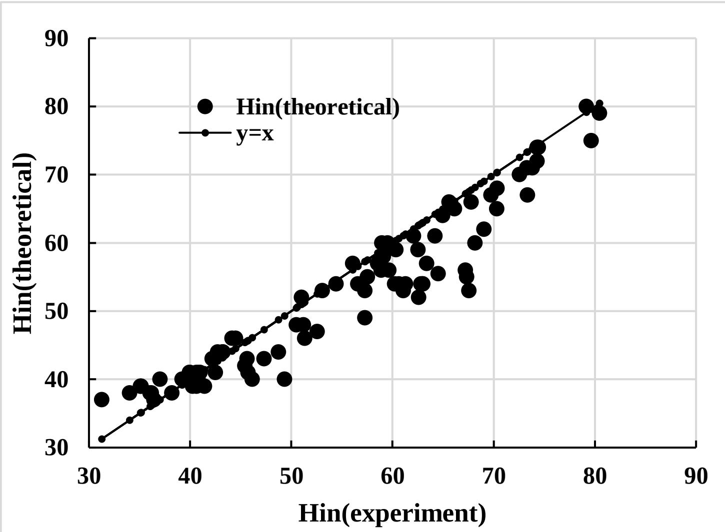

Fig. 4. b. Theoretical drying air humidity versus experimental values

3.3 Results For The Modeling Of Cassava Drying Curve

Table 2. Drying Curve Modeling Results

Models	Constants				Statistical parameters		
	a	k	n	b	R^2	chi-square	RMSE
Newton	---------	0.0624	------	-------	0.8124	0.0993	0.3096
Page	0.000935	2.89	------	--------	0.8659	0.0596	0.2357
Logarithmic	1.8645	0.1395	-------	--------	0.991	0.0026	0.0497
Henderson and Pabis	1.8645	0.1395	0	--------	0.991	0.0027	0.0497
Midili-Kucuk	1.6571	0.05751	1.4088	0.0043	0.997	0.00091	0.0280

Tab. 2 contains the calculated values of the statistical parameters used for the choice of the best model as well as the values of the constants for each model. Among the models used, the Midili-Kucuk model has the highest value of the coefficient of determination (0.996) and the lowest values of the chi-square (0.00148) and the RMSE (0.036). It is therefore the model that best represents the drying curve of the manioc. Fig. 5a presents cassava experimental and numerical moisture content variation versus drying time. We can observe the same evolution for the curves. And on Fig. 5b we also have a good distribution of points around the Y=X line. The best expression of X(t) for the drying curve is, therefore:

$$X(t) = 1.6571exp\,(-0.05751t^{1.40887}) + 0.0043t \quad (26)$$

This new expression of X(t) would allow obtaining theoretical values of the relative humidity of the air closer to the experimental points if inserted in eq. (1).

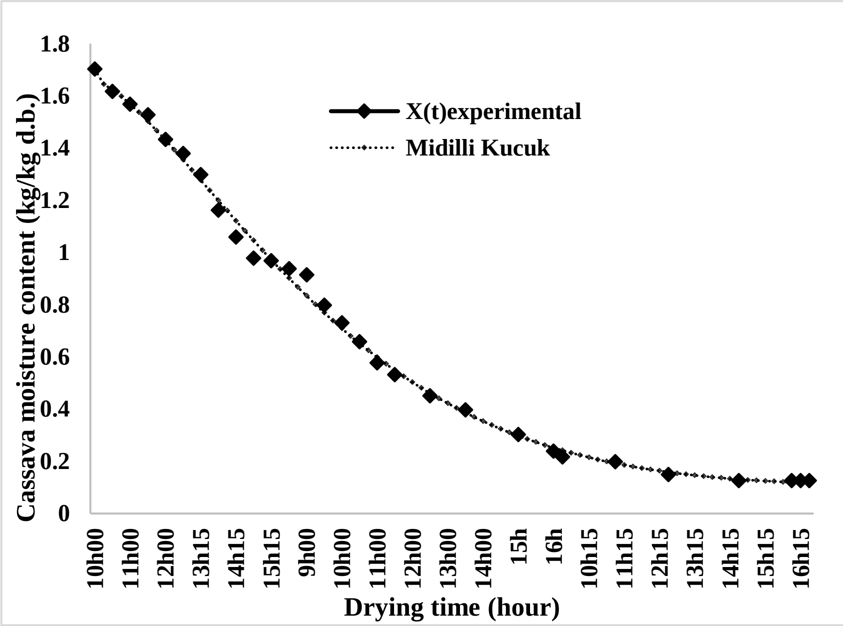

Fig. 5. a. The experimental and numerical moisture content of cassava versus drying time

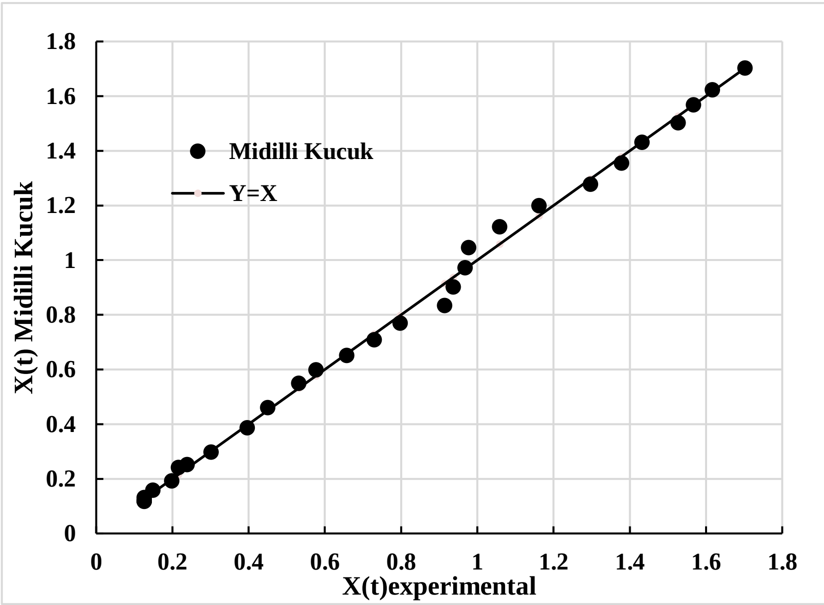

Fig. 5. b. Numerical moisture content versus experimental points

3.4 MASS TRANSFER AND HEAT TRANSFER COEFFICIENTS EVOLUTION

Fig. 6 outlines heat and mass transfer coefficient evolution with the drying time. We observe an increase in their values. They are between 0.00046 and 0. 0017 for the heat transfer coefficient and between 0.000213 and 0.00083 for the mass transfer coefficient. Other researchers observed these same increases earlier in their works [29], [30]. Drying air temperature increases with drying time. This increase of the drying air temperature increases the temperature of the food material, involving thus raising its rate of moisture diffusion from inside to its surface. Then mass transfer coefficient increases with increasing drying air temperature [7]. Since the heat transfer coefficient is calculated in the same way as the mass transfer coefficient, their evolution is almost similar.

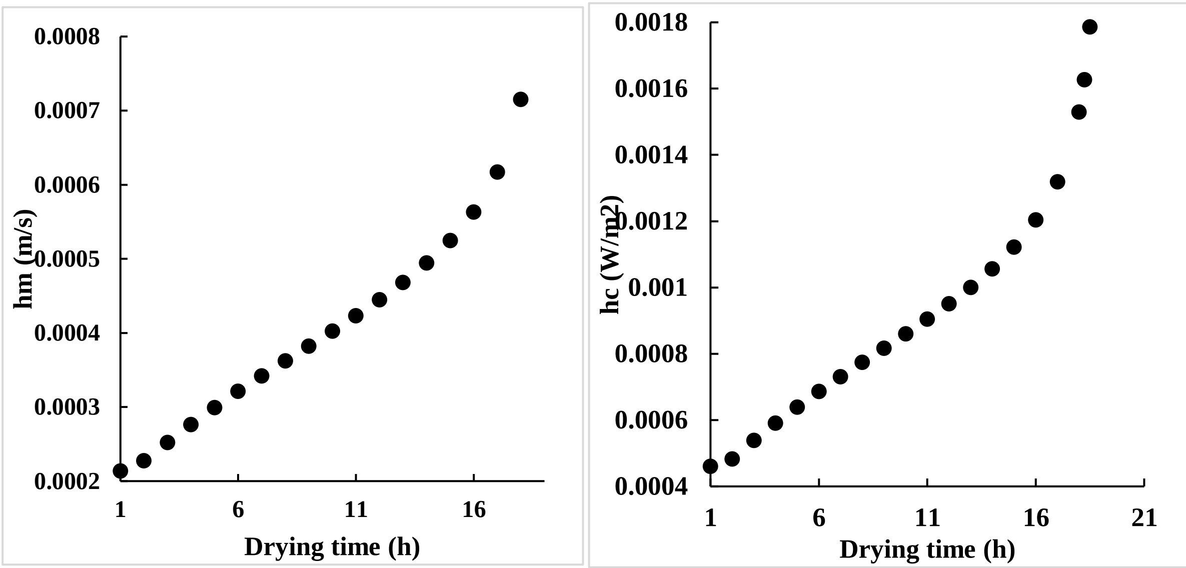

Fig. 6. Evolution of heat and mass transfer coefficient during drying of cassava in the ventilated attic.

3.5 TEMPERATURE EVOLUTION IN THE ATTIC

Tab. 2 presents the values of ambient temperature and that of the attic air during experimentation days. There is a low temperature in the attic compared to outside air temperature at the beginning of the drying. On the third day, the trend is reversed; the outside temperature becomes lower than that in the attic. These findings are in line with those of paragraph 3.1. The first days of drying are marked by the evaporation of the free water of the product. The air in the attic being filled with this moisture, its temperature remains lower than that of ambient air. During this period, only the circulation of the air generated by the chimneys makes it possible to dry. On the last day, moisture becomes rare and difficult to tear out from the product. The air in the attic becomes less wet and its temperature increases during the day with sunshine. The product bed behaves like an additional obstacle preventing the heat captured by the roof from reaching the ceiling. The risk that the heat of the attic passes through the ceiling covered with insulation is therefore very low. When there is no product to dry in the attic, increased air flow generated by chimneys [25] and the insulation on the ceiling impede heat from crossing the ceiling. With this type of attic, there is no heat growth in the underneath room linked to the roof.

Table 3. Temperature evolution inside and outside the attic

Hours	Internal temperature(°C)			External temperature(°C)		
	Day 1	Day 2	Day 3	Day 1	Day 2	Day 3
10:00	29.2	27.21	29.82	29.31	29.31	28.45
10:30	29.59	27.81	31.29	29.89	29.89	29.07
11:00	29.58	28.35	32,52	29.89	29.89	29.34
11:30	29.86	29.05	33.44	30.17	30.17	29.33
12:00	30.13	29.41	32.51	30.44	30.44	29.58
12:30	30.31	29.73	32.52	30.62	30.62	29.85
13:00	30.64	30.14	33.56	30.95	31.14	30.49
13:30	31.2	30.44	34.37	31.51	30.96	30.57
14:00	31.68	30.82	34.76	31.99	31.55	31.06
14:30	31.76	30.56	35.33	32.07	31.68	31.15
15:00	31.66	30.62	36.71	31.97	31.82	31.29
15:30	33.49	30.78	36.26	33.8	32.15	31.74
16:00	32.17	31.84	36.78	32.48	32.24	32.38
16:30	32.52	31.51		32.83	32.21	
17:00	32.96	30.86		33.27	32.54	
17:30	31.89	30.51		32.2	32.68	
18:00	31.87	30.21		32.18	32.93	

4 CONCLUSION

A prototype of ventilated attic usable for the drying of the products is built and tested with the drying of cassava in Yamoussoukro. To have a clear idea of the variation of moisture in the air of the attic and the product, a mathematical model of mass transfer is developed for air humidity and the drying curve is modeled with five semi-empirical equations. Simulation of the mass transfer model gives satisfactory results. Indeed, the mean relative deviation modulus (E%) gives a value consistent with the recommendation of the literature. For the drying curve, the model that gives a higher value of the determination coefficient and low values of the chi-square and the RMSE is the model of Midili-Kucuk. Increases in heat and mass transfer coefficients with drying time were observed too. The values ranged between 0.00046 and 0.0017 for the heat transfer coefficient and between 0.000213 and 0.00083 for the mass transfer coefficient. This attic also prevents the heat captured by the roof from migrating into the room below by the ceiling, thus contributing to thermal comfort. We envisage a comparative study of its behavior in the rainy season and the dry season and with other agricultural products.

NOMENCLATURE

C_p : specific heat [$Jkg^{-1}K^{-1}$];
h_c : heat transfer coefficient [$Wm^{-2}.K^{-1}$];
h_m : mass transfer coefficient [m/s];
Hr : air relative humidity [%]
L_v : latent heat of evaporation of water [J/kg];
m: air mass, product mass [kg]
$\dot{m}$: mass flow rate [kg/s],
$Ps(T)$: pressure of saturated air [mmHg]
P : atmospheric pressure [Pa];
S: surface [m^2];
T: temperature [k];
t: time [s];
X: product moisture content in dry bases [kg/kg];
$\dot{X}$: Product moisture flow rate [$kgkg^{-1}s^{-1}$]
Y : air humidity [kg/kg];
$Y' = \frac{dY}{dt}$: air humidity flow rate[$kgkg^{-1}s^{-1}$];
Z : altitude of the place [m];

Greek symbole

ρ_a : air density [kg/m^3]

Subscripts

a: air
e: ambient air
p: product
s: drying air, product surface
exp: experimental
theo: theoretical
0: anhydrous

REFERENCES

[1] Macmanus Chinenye Ndukwu, O.A. Akani, K.J. Simonyan, "Nigeria's grain resource structure, and government sustainable policy: A review", Agric. Eng. Int. CIGR J, vol. 3, no. 17, pp. 441–457, 2015.
[2] http://www.fao.org/docrep/008/w0078f/w0078f0c.
[3] Mohammed, B., et Al., "Profitability in chili pepper production in Kaduna state, Nigeria", Br. J. Appl. Sci. Technol., Vol. 3, no 12 pp. 1-9, 2016.
[4] Koua, K. B., et Al., "Modeling of thermal behavior of a direct solar drier possessing a chimney: Application to the drying of cassava", Indian Journal of Science and Technology, vol. 4, no. 12 pp. 1609-1618, 2011.
[5] Dissa, A. O., et Al., "Modeling and experimental validation of thin layer indirect solar drying of mango slices", Renew. Energy, vol. 4, no. 34, pp. 1000-1008, 2009.
[6] Koua Kamenan Blaise, Ekoun Paul Magloire and Prosper Gbaha, Séchage des fèves de cacao dans un séchoir solaire indirect à circulation forcé d'air , CAMES journal - Applied and Engineer Sciences, vol. 2, no.2, pp. 15-19, 2017.
[7] Koua Kamenan Blaise, Ekoun Paul Magloire and Prosper Gbaha, "Evolution of shrinkage, real density, porosity, heat, and mass transfer coefficients during indirect solar drying of cocoa beans", Journal of the Saudi Society of Agricultural Sciences, vol. 18, no. 1, pp. 72-82, 2019.
[8] Kanyarusoke, K. E., "An Engineered solar crop and meat dryer for rural Africa: A techno-economic outlook", IOP Conf. Series: Earth and Environment Science, vol. 354, no. 012009, pp. 402-409, 2019.
[9] Udomkun, P., et Al., "Review of a solar dryer for agricultural products in Asia and Africa: an innovation landscape approach", Journal of Environment Management, vol. 268, no. 110730, 2020.
[10] Brian Norton, "Characteristics of different systems for the solar Drying of Crops", Solar Drying Technology Springer, vol. 10, no 4, pp. 978-981, 2017.
[11] Onwude, D. I., et Al., "Modeling the thin layer drying of fruits and vegetables: a review", Compr. Rev. Food Sci. Food Saf., vol. 15 , pp. 599-618, 2016.
[12] Simo-Tagne, M., et Al., "Modeling, numerical simulation and validation of a convective dryer in steady conditions: a case study of tropical woods", Int. J. Model. Simul., 2019.
[13] B. Lamrani, A. Khouya, B. Zeghmati, A. Draoui, "Mathematical modeling and numerical simulation of a parabolic trough collector: a case study in thermal engineering", Therm. Sci. Eng. Prog., vol. 8, pp. 47-54, 2018.
[14] Henriquez, C., et Al., "Kinetic modeling of phenolic compound degradation during drum-drying of apple peel by products", J. Food Eng., vol. 143, pp. 146-153, 2014.
[15] Simo-Tagne, M., et Al., "Numerical analysis and validation of a natural convection mix-mode solar dryer for drying red chili under variable conditions", Renewable Energy, vol. 151 , pp. 659–673, 2020.
[16] Fokone, T. A., et Al., "Modélisation de la Cinétique de Séchage de la Carotte(Daucus carota), International Journal of Innovation and Applied Studies, vol. 4, no. 2, pp. 375-381, 2013.
[17] Koffi A. S., et Al., "A numerical model of cocoa beans drying kinetics in an indirect solar and air crossing dryer", International Journal of Innovation and Applied Studies, vol. 23, no. 4, pp. 717-731, 2018.
[18] Bassene, P. T., et Al., " Détermination expérimentale et modélisation de la cinétique de séchage des granules de la farine de mil par la méthodede la courbe caractéristique de séchage (CCS) '', AfriqueSCIENCES, vol. 13, no. 4, pp. 241-250, 2017.
[19] Simo-Tagne, M., et Al., "Numerical Study of the Drying of Cassava Roots Chips Using an Indirect Solar Dryer in Natural Convection", AgriEngineering, vol. 3, pp. 138–157, 2021.
[20] Merlin Simo-Tagne & Lyes Bennamoun, "Numerical study of timber solar drying with application to different geographical and climatic conditions in Central Africa", Solar Energy, vol. 170, pp. 454-469, 2018.
[21] Naoual Bekkioui, Séchage solaire du bois: modélisation simplifiée du séchage solaire d'une pile de bois dans un séchoir solaire à parois vitrées, Thèse de Doctorat, Université Mohammed V-AGDAL, Rabat, Maroc, 2009.
[22] Siaka Toure & Serges Kibangu-Nkembo, "Comparative study of natural solar drying of cassava, banana, and mango", Renewable Energy, vol. 29, pp. 975–990, 2004.
[23] Koua, K. B., et Al., "Etude expérimentale de la cinétique de séchage du manioc dans un séchoir solaire directe muni d'un circulateur thermique". Rev. Ivoire sci. Technol., vol. 9, pp. 11-26, 2007.
[24] Galilée, L. P., L'air humide, Academie de Paris, Paris, France, 2005.
[25] Tieu, Z. A., et Al., "Étude expérimentale d'un grenier séchoir solaire à convection naturelle: Application au séchage du cacao et du manioc", AfriqueSCIENCES, vol. 2, no. 15, pp. 80 – 95, 2019.
[26] Danny S. Parker, Improving Attic Thermal Performance, 2004. [online] Available: http://www.homeenergy.org. (Jun 8, 2020).
[27] Pechaporn, P., et Al., "Effect of temperature and shape on drying performance of cassava", Agriculture and Natural Resources, vol. 51, pp. 402-409, 2017.
[28] Rosa GS Moraes MA & Pinto, "Moisture sorption properties of chitosan", LWT-Food Sci. vol. 43, pp. 415-420, 2010.
[29] Fu, B. A., et Al., "Heat transfer characteristics on lignite thin layer during hot air forced convective drying", Fuel, vol.154, pp. 132-139, 2015.
[30] Ateeque, M., et Al., "Numerical modeling of convective drying of food with spatially dependent transfer coefficient in a turbulent flow field", *int. J. Therm. Sci, vol. 78,* pp. 145-157, 2014.